Available online at www.sciencedirect.com
SCIENCE DIRECT®
International Journal of Mass Spectrometry 229 (2003) 231–240
International Journal of Mass Spectrometry
www.elsevier.com/locate/ijms

A selected ion flow tube study of the reactions of H_3O^+, NO^+ and O_2^+ with a series of monoterpenes

N. Schoon [a,*], C. Amelynck [a], L. Vereecken [b], E. Arijs [a]

[a] *Belgian Institute for Space Aeronomy, Ringlaan 3, B-1180 Brussels, Belgium*
[b] *Department of Chemistry, University of Leuven, Celestijnenlaan 200F, B-3001 Heverlee, Belgium*

Received 4 June 2003; accepted 25 July 2003

Abstract

The ion/molecule reactions of H_3O^+, NO^+, and O_2^+ with six monoterpenes (α-pinene, β-pinene, limonene, Δ^3-carene, myrcene, and camphene) have been studied at 298 K and 1.47 mbar using a selected ion flow tube (SIFT). The rate constants and the ionic products of the reactions have been determined. It turns out that all reactions occur at the collisional rate. Quantum chemical calculations were performed of the polarizability and dipole moments of all six monoterpenes studied, to determine the collisional rate constant using the Su–Chesnavich approach. Our results show that the H_3O^+ reactions with the monoterpene M proceed via proton transfer and result in the protonated molecules MH^+ ($m/z = 137$) and partly in an ion with $m/z = 81$. The NO^+ reactions proceed via charge transfer resulting mainly in the ionized monoterpene $C_{10}H_{16}^+$. The reactions with O_2^+ proceed via dissociative charge transfer giving rise to several ionic products, which have also been observed in electron impact spectra of these monoterpenes.

Keywords: SIFT; Ion/molecule reactions; Proton transfer; Monoterpenes

1. Introduction

Monoterpenes ($C_{10}H_{16}$) are important constituents of biogenic volatile organic compounds that are emitted by vegetation in large quantities. Their global emission has been studied by several authors [1–3] and is estimated to be 127 MT C per year [4]. Due to their high reactivity with some atmospheric components such as O_3 and the radicals OH and NO_3 these compounds play an important role in the chemistry of the troposphere [5,6]. The atmospheric oxidation of monoterpenes leads to a variety of products [7] and contributes significantly to the formation of so called secondary organic aerosols [8] in the troposphere.

Monoterpenes have been detected and quantified in the laboratory and in the atmosphere by several techniques mainly consisting of preconcentration steps, such as cryosampling or adsorption on suitable sorbent tubes, followed by GC–MS [2,9,10].

Recently, proton transfer mass spectrometry (PTR-MS) has also been used for the measurement of monoterpenes in several field campaigns [11–13]. This method, which is based on the high reactivity of the H_3O^+ ion with the trace gas to be measured [14], requires a good knowledge of the reaction rate constants and product distributions of H_3O^+ with the different monoterpenes. Only recently these data were obtained for the monoterpenes α-pinene, β-pinene, Δ^3-carene, and limonene under typical PTR-MS conditions [15].

In the present study, we have investigated the reaction of H_3O^+ with the same monoterpenes, with the addition of myrcene and camphene, in a selected ion flow tube (SIFT). Moreover, we studied the reactions of NO^+ and O_2^+ with the six monoterpenes α-pinene, β-pinene, Δ^3-carene, limonene, myrcene, and camphene.

Whereas this study has originally been made in support of the laboratory measurements undertaken at our institute to study the OH-initiated oxidation of α-pinene in the presence of O_2 and NO, using a neutral fast flow reactor coupled to a chemical ionization mass spectrometer [16], it also investigates the feasibility of using H_3O^+, NO^+ or O_2^+ as primary ion for the detection of monoterpenes through the selected

* Corresponding author. Tel.: +32-2373-0391; fax: +32-2374-8423.
E-mail address: Niels.Schoon@bira-iasb.oma.be (N. Schoon).

1387-3806/$ – see front matter © 2003 Elsevier B.V. All rights reserved.
doi:10.1016/S1387-3806(03)00343-9

ion flow tube-mass spectrometry (SIFT-MS) method, which has been applied successfully by Smith and co-workers in a number of medical applications [17–19].

Very recently kinetic data of the H_3O^+, NO^+, and O_2^+ reactions with 11 monoterpenes have been reported by Wang et al. [20], obtained from assumed collisional rate constants for H_3O^+ and relative measurements for NO^+ and O_2^+, whereas in this study the results for H_3O^+ were obtained from absolute measurements.

2. Experimental

The experimental set-up used in the present study is a new SIFT, which has recently been developed, based upon the original design by Smith and Adams [21]. It is shown schematically in Fig. 1. The major parts are: an ion source, an ion selection and injection system, a flow tube and an ion detection mass spectrometer.

Source ions are produced by generating a microwave discharge in a mixture of air and water vapor at a total pressure of 0.21 mbar, using an Evenson type cavity operating at 2.45 GHz and 40 W. The ions are extracted from the discharge through a biased plate with a hole of 2 mm, which separates the ion source from the SIFT chamber, consisting of two separate parts. The first chamber contains the ion lenses and is pumped by a 1600 l s^{-1} turbomolecular pump. The second chamber, built into the first one, houses the selection mass spectrometer and is pumped by a 500 l s^{-1} turbomolecular pump. An electrostatic five element ion lens focuses the ions into the differentially pumped quadrupole mass spectrometer, where the appropriate ion (H_3O^+, NO^+ or O_2^+) is selected. The ion selection mass filter consists of a quadrupole assembly with a rod diameter of 12 mm and a total length of 275 mm (20 mm pre-filter, 230 mm main filter and 20 mm post-filter). The mass selected ions are focused by a second electrostatic three element lens towards the SIFT injector, which is constructed according to the Birmingham design [22] and which has a central hole of 0.75 mm, through which the ions reach the flow tube, and a circular array of 12 holes with a diameter of 0.70 mm, through which the main carrier gas flow is sent into the flow tube.

The flow tube is made of stainless steel and has a diameter of 40 mm and a total length of 50.7 cm (from injection point to ion inlet plate). Three gas inlets are provided, two of which are used for reaction gas introduction and one for mass discrimination effect calibrations, as described later.

Ions are convectively transported using a main carrier helium gas flow of 100 STP cm^3 s^{-1}, resulting in a pressure of 1.47 mbar in the flow tube. All experiments were performed at this pressure. Small amounts of nitrogen were added a few cm downstream to the helium main flow to quench possible excited states of the source ions. The main carrier gas flow is maintained by a large Roots blower of 500 m^3 h^{-1} backed by a rotary vane pump of 120 m^3 h^{-1}. At the downstream end of the flow tube, the ions are sampled through a 0.4 mm hole, drilled into a conically shaped biased inlet flange. An electrostatic lens focuses the ions into the analyzer quadrupole consisting of four rods of 200 mm length with a diameter of 8 mm. After mass filtering the ions are detected by

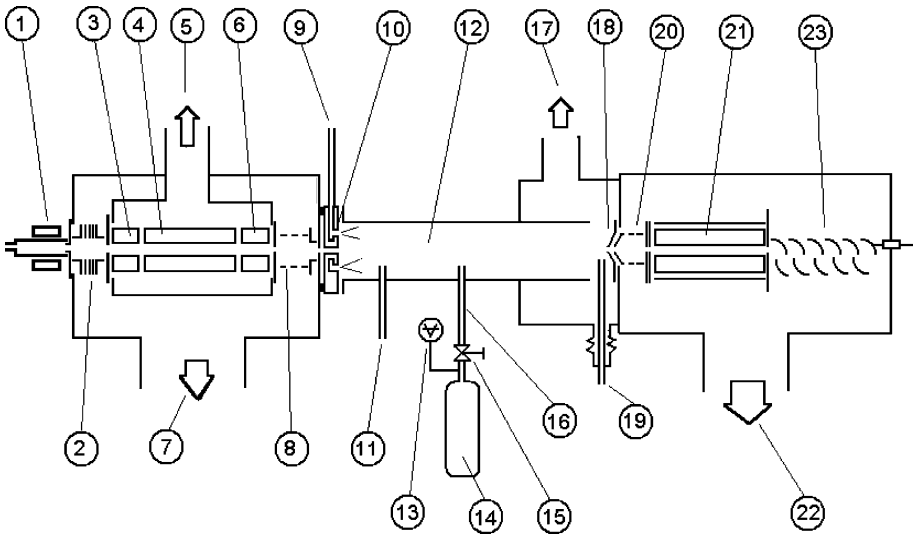

Fig. 1. Schematic representation of the SIFT instrument: (1) microwave discharge ion source; (2) ion inlet lens; (3) selection quadrupole pre-filter; (4) selection quadrupole main filter; (5) to 500 l s^{-1} turbomolecular pump; (6) selection quadrupole post filter; (7) to 1600 l s^{-1} turbomolecular pump; (8) exit ion lens; (9) inlet main carrier gas; (10) SIFT venturi inlet; (11) reactant gases inlet for mass discrimination measurements; (12) flow tube; (13) pressure gauge (baratron); (14) calibrated volume with mixture monoterpene/helium; (15) needle valve; (16) reactant gas inlet; (17) to Roots blower; (18) biased ion inlet flange; (19) reactant gas inlet for measurement of the branching ratio of the reaction product ions; (20) ion inlet lens; (21) quadrupole analyzer; (22) to turbomolecular pumping system; (23) electron multiplier.

an electron multiplier, the signals of which are treated by pulse counting techniques. The analyzer quadrupole housing is pumped by four turbomolecular pumps of 300 l s^{-1}, mounted on four sides of the cubic chamber.

To determine the ion/molecule reaction rate constant k, the source ion signal I was measured as a function of the concentration of the reactant neutral in the flow tube [X]. From the logarithmic decay $\ln(I/I_o) = -k\tau[X]$, k can then be derived if the residence time τ of the ions in the flow tube is known.

In a first set of experiments, the reactant neutrals were introduced through an electrically insulated finger inlet, located at 27 cm from the ion inlet plate. With this inlet the ion residence time τ was determined by applying a positive voltage pulse on the insulated finger inlet and by simultaneously recording the arrival of the disturbance of the ion swarm on the ion detector. To vary the concentration of the neutral reactant, volumetric mixtures (manometrically diluted) of the different monoterpenes in helium were prepared, and introduced via a flowmeter/controller.

For the measurement of the reaction rate constant of H_3O^+, NO^+, and O_2^+ two different methods were used. Either H_3O^+, NO^+, and O_2^+ were injected simultaneously (putting the ion selection quadrupole in the total ion mode) and their signals were measured as a function of the reactant gas flow or the upstream quadrupole was programmed to switch subsequently between H_3O^+, NO^+, and O_2^+ at each value of the neutral reactant flow.

It turned out, however, that the results obtained using the flowmeter/controller were not reproducible, because the flowmeter gave irreproducible results for the reactant gas flow, most probably due to the sticky nature of the monoterpenes. Nevertheless, the relative decay rates of the three ion species, obtained in this way, can be used to derive the rate constants if one of the three k values is known. This procedure has been applied in many previous studies by Španěl and co-workers, where they assume that for the H_3O^+ reactions [23–35], or the O_2^+ reactions [35,36], k equals the collisional rate k_C, which can in most cases be calculated with the Su and Chesnavich [37,38] approach. In all of these cases this assumption was justified by the fact that either the H_3O^+ proton transfer reactions were exothermic, because the proton affinity of the reactant molecules was larger than the proton affinity of water [23–35], or by available data on the reactions of O_2^+ with similar molecules [35,36]. Unfortunately, no data are available for the proton affinities of the monoterpenes studied, except for limonene [39], and therefore, we cannot assume in all cases that $k = k_C$ for the H_3O^+ reactions studied here. Furthermore, no data are available for the O_2^+ reactions with monoterpenes and although for some of the monoterpenes the ionization energy is smaller than the one for O_2 and NO, the exothermic reactions with O_2^+ and NO^+ do not necessarily proceed at the collision rate. We, therefore, cannot rely upon the knowledge of k for one of the three ion/molecule reactions (H_3O^+, O_2^+ or NO^+) to derive the other two in our case. Recently, some of the H_3O^+ proton transfer reactions with four of the monoterpenes, studied here, were measured in a PTR-MS [15]. These PTR-MS data, however, were not available at the time we started our experiments and therefore, we decided to try to perform some absolute measurements of k for the H_3O^+ reactions.

Reproducible results have been obtained by flowing volumetric mixtures of the terpene in helium, prepared in volume calibrated glass containers, into the flow tube through a needle valve heated at 40 °C. From the pressure decay versus time in the glass containers the gas flow could be determined. For each terpene four different mixing ratios of the volumetric mixtures were used and each of those resulted in the same k value within 5%. For the absolute reaction rate constant measurements of H_3O^+, a ring shaped inlet with six holes, oriented against the main carrier gas flow, has lead to the best results, giving minimum end effects. Since this ring shaped inlet was not electrically insulated, no measurements of the ion residence time τ were possible with it. We, therefore, had to rely upon the measurements of τ performed before with the finger inlet. The validity of this procedure was checked by measuring the reaction rate constant of H_3O^+ with acetone with the ring inlet and using the ion residence time previously determined with the finger inlet. A value of 3.8×10^{-9} molecule^{-1} cm^3 s^{-1} was found in perfect agreement with the literature data [23].

For the determination of the product ion branching ratios of the different ion/molecule reactions a second reaction gas inlet, located at 8 mm from the ion inlet plate, is used. This inlet consists of a stainless steel tube with an outer and inner diameter of 4 and 2 mm, respectively and is mounted with the aid of a small bellow, so that it can either be put directly in front of the ion inlet hole during the product distribution measurements to eliminate diffusion enhancement effects [40], or be removed, by shifting it backwards, during the reaction rate measurements.

Although diffusion enhancement effects can be eliminated by using this inlet close to the sampling hole, the mass discrimination of the downstream mass spectrometer still has to be accounted for. To do so a third gas inlet is used, located 10 cm downstream from the ion injection point. Through this calibration inlet a number of gases such as acetone, pentanone, butanone and benzene can be introduced to measure the mass discrimination in the way described by Španěl and Smith [40]. These measurements are done on a regular base to take into account aging of the electron multiplier used in the ion detection mass spectrometer system.

The monoterpenes used here were all obtained commercially. α-Pinene, β-pinene, Δ^3-carene, and camphene (Aldrich) were 99, 99, 99, and 95% pure, respectively. Limonene (Fluka) was 99% pure and myrcene (Merck) 85%. The He carrier gas (Air Products) was GC quality (99.9995%) and the N_2 (Air Products) was 6.0 quality (99.9999%).

3. Results

3.1. Reaction rate constants

The experimentally derived reaction rate constants k_{exp} for the H_3O^+, NO^+, and O_2^+ reactions with the six monoterpenes are shown in Table 1. The k_{exp} values for the H_3O^+ reactions were derived in an absolute way from the decay of the source ion signal versus monoterpene concentration, inferred from absolute flow rates, which were obtained by monitoring the pressure decrease of a known volume of the monoterpene/helium mixture, as described in Section 2. The reaction rate constants for the NO^+ and O_2^+ reactions were measured relatively with respect to the one of H_3O^+ by recording the decay of the three source ions simultaneously (or subsequently) with increasing concentration of the monoterpene, introduced into the flow tube via a flowmeter/controller.

The accuracy of the experimental rate constants shown in Table 1 is estimated to be 20% with a precision better than 5%.

Fig. 2 shows a typical example of the decay of the count rates for the three source ions versus the concentration of the reactant neutral.

Also listed in Table 1 are the collision rate constants k_C calculated with the parameterized equation of Su and Chesnavich [37,38], based upon trajectory calculations:

$$k_C = k_L C(\alpha, \mu_D, T), \quad (1)$$

where k_L is given by the Langevin formula:

$$k_L = 2\pi q \sqrt{\frac{\alpha}{\mu}}, \quad (2)$$

with q the absolute value of the charge of the ion, α and μ_D, respectively, the polarizability and the dipole moment of the ion and μ the reduced mass of the ion/molecule system (all

Table 1
Polarizability, dipole moment and reaction rate constants of the monoterpenes

Molecule	α (Å^3)	μ_D (Debye)	k_{exp}, k_C, $k_{ref.[15]}$ (H_3O^+)	k_{exp}, k_C (NO^+)	k_{exp}, k_C (O_2^+)
α-Pinene	17.3	0.177	2.3 [2.4] 2.2	2.0 [2.0]	2.0 [1.9]
β-Pinene	17.5	0.742	2.4 [2.6] 2.3	2.1 [2.2]	2.1 [2.1]
Limonene	18.3	0.599	2.6 [2.6] 2.3	2.2 [2.2]	2.2 [2.1]
Δ^3-Carene	17.6	0.168	2.3 [2.4] 2.2	2.1 [2.0]	2.0 [2.0]
Myrcene	19.8	0.582	2.6 [2.7]	2.3 [2.2]	2.2 [2.2]
Camphene	17.2	0.673	2.4 [2.6]	2.1 [2.1]	2.0 [2.1]

Polarizability α and dipole moment μ_D of the monoterpenes obtained from quantum chemical calculations. Experimental determined rate constants k_{exp} for the reactions of H_3O^+, NO^+, and O_2^+ with the monoterpenes and in square brackets their corresponding collisional rate constants k_C, calculated with the method of Su and Chesnavich, based upon trajectory calculations. Also listed are the PTR-MS results [15] for α-pinene, β-pinene, limonene, and Δ^3-carene. Rate constants are expressed in 10^{-9} molecule^{-1} cm^3 s^{-1}.

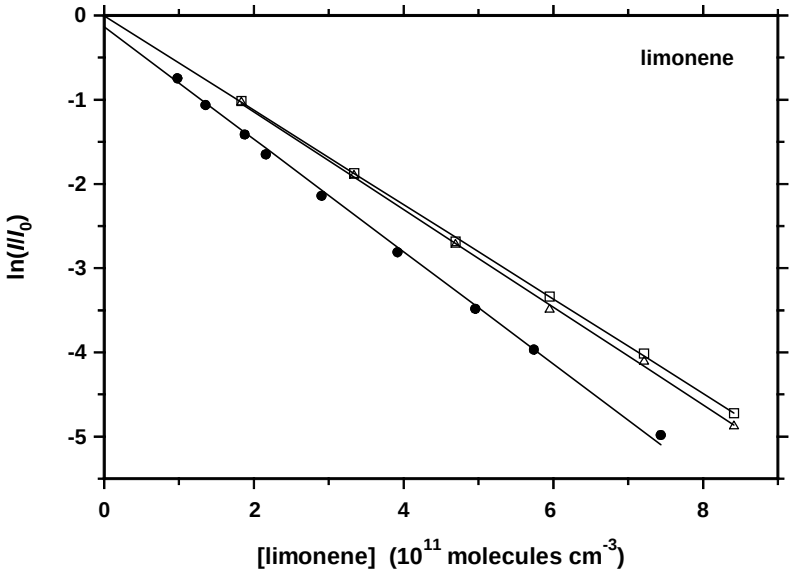

Fig. 2. Semi-logarithmic decay of the source ion signal vs. limonene concentration in the flow tube. (●) H_3O^+; (△) NO^+; (□) O_2^+. Limonene concentrations for the H_3O^+ signal were derived in an absolute way (pressure decay of a known volume), whereas for the NO^+ and the O_2^+ signal, which were measured in another experiment, the limonene concentration was derived from the H_3O^+ signal measured simultaneously (but not shown on the graph), and the k_{exp} (H_3O^+) derived from the above mentioned absolute measurement.

variables in atomic units). C is a parameterized equation, depending upon α, μ_D, and temperature T.

As far as we know, no information is available for the dipole moment and polarizability of the monoterpenes, except estimations based upon known values for similar molecules [15]. The values for α and μ_D, which should allow us to evaluate k_C, were estimated by quantum chemical calculations at the B3LYP-DFT level of theory using the large aug-cc-pVDZ basis set. The results of these calculations are also shown in Table 1; the accuracy of these calculations is sufficiently high to ensure that the resulting errors are minor compared to the experimental uncertainty. All calculations were carried out using the Gaussian software suite [41].

As can be seen from this table, all reactions proceed within the experimental error at the collision rate. The latter was expected for limonene, which has a proton affinity of $875 \pm 5\,\mathrm{kJ\,mol^{-1}}$ [39], considerably larger than that of water ($691\,\mathrm{kJ\,mol^{-1}}$ [42]), and therefore should result in exothermic proton transfer, which is expected to proceed at the collision rate. The rate constants for the H_3O^+ reaction obtained in this work are also in good agreement with those derived by Tani et al. [15].

3.2. Product distributions

An overview of the products of the reactions of H_3O^+, NO^+, and $O_2{}^+$ with the monoterpenes, as observed using the reactant gas inlet close to the ion inlet plate (see Section 2), is given in Table 2. Only those ions which represent more than 1% of the product ion distribution are listed. Product ions with a smaller yield are included in "others". It should be noted that the accuracy of the branching ratios is mainly determined by the error on the mass discrimination measurements, which are performed at the end of each day of product distribution measurements, and for products with small branching ratios by the statistical error on their count rate. The accuracy is estimated to be 20% for branching ratios higher than 5%, and gradually increases up to 25% for branching ratios of the order of 1%.

3.2.1. H_3O^+ reactions

The reaction of H_3O^+ with all six monoterpenes mainly results in a product with $m/z = 137$, through proton transfer, and to a lesser degree in a product ion with $m/z = 81$.

$$H_3O^+ + C_{10}H_{16} \rightarrow C_{10}H_{17}{}^+ + H_2O \quad (3)$$

$$H_3O^+ + C_{10}H_{16} \rightarrow C_6H_9{}^+ + \text{products}. \quad (4)$$

Minor ions with smaller branching ratios are also observed at $m/z = 69$ (for myrcene), 93 (in the case of α-pinene and myrcene) and 95 (for β-pinene, limonene and myrcene) as fragments of the nascent $(C_{10}H_{17}{}^+)^*$ excited product ion formed in the initial protonation step.

The product ions with $m/z = 137$ and 81 have been observed previously in SIFT-MS spectra for limonene by Španěl and Smith [43] and for α-pinene and β-pinene in PTR-MS experiments [12,13,15]. Tani et al. [15] report the observation of some of the minor product ions, besides those with $m/z = 137$ and 81, but they suggest that a fraction of the signal at $m/z = 93$ could originate from unknown impurities in the monoterpene standards.

For the determination of the product distribution, the concentration of the monoterpene in the flow tube, introduced by means of the finger inlet in front of the ion inlet plate, is kept as low as possible, with the only restriction that reasonable count rates for the different product ions are obtained. Typically a flow of $1.7\,\mathrm{STP\,cm^3\,s^{-1}}$ of a 0.1% diluted mixture of the monoterpenes in He is used.

Although the ion residence time in the flow tube is very short, small signals of secondary product ions $(C_{10}H_{17}{\cdot}C_{10}H_{16})^+$ and $(C_6H_9{\cdot}C_{10}H_{16})^+$ have been observed, possibly formed through clustering:

$$C_{10}H_{17}{}^+ + C_{10}H_{16} + He \rightarrow (C_{10}H_{17} \cdot C_{10}H_{16})^+ + He \quad (5)$$

and

$$C_6H_9{}^+ + C_{10}H_{16} + He \rightarrow (C_6H_9 \cdot C_{10}H_{16})^+ + He \quad (6)$$

As can be seen from Fig. 3, which shows the development of the product ions at $m/z = 81$ ($C_6H_9{}^+$), 93 ($C_7H_9{}^+$), 95 ($C_7H_{11}{}^+$) and 137 ($C_{10}H_{17}{}^+$) as a function of the monoterpene concentration for α-pinene, when the reactant is introduced through the ring inlet at 27 cm from the ion inlet plate,

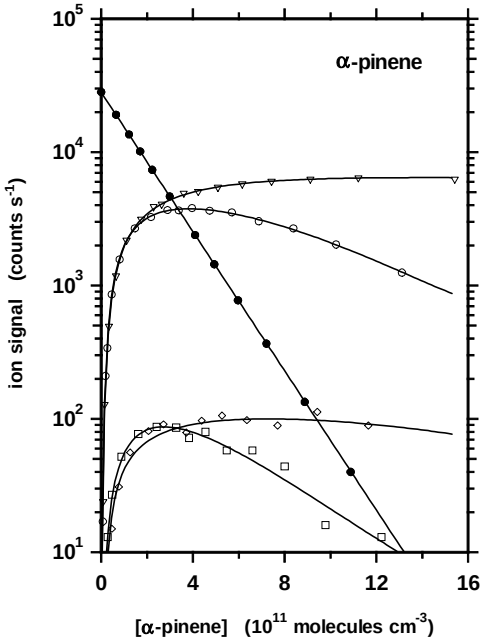

Fig. 3. Evolution of the source and product ions for the reaction of H_3O^+ with α-pinene versus the concentration of the monoterpene. (●) H_3O^+; (○) $m/z = 81$; (□) $m/z = 93$; (◇) $m/z = 95$; (▽) $m/z = 137$. α-Pinene was introduced through a flowmeter/controller at the reaction inlet 27 cm upstream from the ion inlet plate. The concentration of the monoterpene was derived from the decay of the H_3O^+ signal and the knowledge of the reaction rate constant of H_3O^+ and the ion residence time. Signals were not corrected for mass discrimination nor for diffusion enhancement.

Table 2
Products of the reactions of H_3O^+, NO^+, and O_2^+ with the monoterpenes and their corresponding branching ratio

Molecule	H_3O^+			NO^+			O_2^+		
	Product	*m/z*	%	Product	*m/z*	%	Product	*m/z*	%
α-Pinene 8.07[a]	$C_6H_9^+$	81	30	$C_7H_8^+$	92	8	$C_6H_8^+$	80	3
	$C_7H_9^+$	93	1	$C_7H_9^+$	93	4	$C_7H_8^+$	92	18
	$C_{10}H_{17}^+$	137	67	$C_{10}H_{16}^+$	136	85	$C_7H_9^+$	93	52
	Others		2	$(NO{\cdot}C_{10}H_{16})^+$	166	1	$C_7H_{10}^+$	94	2
				Others		2	$C_8H_{11}^+$	107	3
							$C_8H_{12}^+$	108	1
							$C_9H_{13}^+$	121	12
							$C_{10}H_{16}^+$	136	6
							Others		3
β-Pinene	$C_6H_9^+$	81	33	$C_7H_8^+$	92	1	$C_5H_9^+$	69	2
	$C_7H_{11}^+$	95	1	$C_7H_9^+$	93	3	$C_6H_7^+$	79	1
	$C_{10}H_{17}^+$	137	64	$C_{10}H_{16}^+$	136	93	$C_6H_8^+$	80	4
	Others		2	Others		3	$C_7H_8^+$	92	4
							$C_7H_9^+$	93	56
							$C_7H_{10}^+$	94	6
							$C_8H_{11}^+$	107	3
							$C_8H_{12}^+$	108	1
							$C_9H_{13}^+$	121	9
							$C_{10}H_{16}^+$	136	11
							Others		3
Limonene 8.3[a]	$C_6H_9^+$	81	22	$C_7H_8^+$	92	1	$C_5H_8^+$	68	6
	$C_7H_{11}^+$	95	3	$C_9H_{13}^+$	121	1	$C_6H_8^+$	80	4
	$C_{10}H_{17}^+$	137	73	$C_{10}H_{15}^+$	135	2	$C_6H_9^+$	81	2
	Others		2	$C_{10}H_{16}^+$	136	91	$C_7H_8^+$	92	7
				$(NO{\cdot}C_{10}H_{16})^+$	166	1	$C_7H_9^+$	93	26
				Others		4	$C_7H_{10}^+$	94	11
							$C_7H_{11}^+$	95	3
							$C_8H_{11}^+$	107	9
							$C_8H_{12}^+$	108	3
							$C_9H_{13}^+$	121	14
							$C_{10}H_{16}^+$	136	11
							Others		4
Δ^3-Carene 8.4[a]	$C_6H_9^+$	81	19	$C_7H_8^+$	92	3	$C_6H_7^+$	79	1
	$C_{10}H_{17}^+$	137	78	$C_7H_9^+$	93	4	$C_6H_8^+$	80	6
	Others		3	$C_{10}H_{15}^+$	135	3	$C_7H_8^+$	92	8
				$C_{10}H_{16}^+$	136	86	$C_7H_9^+$	93	41
				$(NO{\cdot}C_{10}H_{16})^+$	166	1	$C_7H_{10}^+$	94	2
				Others		3	$C_8H_{11}^+$	107	4
							$C_8H_{12}^+$	108	1
							$C_9H_{13}^+$	121	20
							$C_{10}H_{16}^+$	136	14
							Others		3
Myrcene	$C_5H_9^+$	69	3	$C_6H_8^+$	80	2	$C_5H_9^+$	69	8
	$C_6H_9^+$	81	26	$C_7H_8^+$	92	8	$C_6H_7^+$	79	2
	$C_7H_9^+$	93	1	$C_7H_9^+$	93	22	$C_6H_8^+$	80	3
	$C_7H_{11}^+$	95	8	$C_7H_{10}^+$	94	1	$C_7H_8^+$	92	3
	$C_{10}H_{17}^+$	137	59	$C_9H_{13}^+$	121	1	$C_7H_9^+$	93	61
	Others		3	$C_{10}H_{15}^+$	135	1	$C_7H_{10}^+$	94	4
				$C_{10}H_{16}^+$	136	61	$C_8H_{11}^+$	107	3
				$(NO{\cdot}C_{10}H_{16})^+$	166	1	$C_8H_{12}^+$	108	1
				Others		3	$C_9H_{13}^+$	121	7
							$C_{10}H_{16}^+$	136	4
							Others		4
Camphene ≤8.86[a]	$C_6H_9^+$	81	9	$C_9H_{13}^+$	121	2	$C_5H_8^+$	68	1
	$C_{10}H_{17}^+$	137	88	$C_{10}H_{16}^+$	136	87	$C_6H_7^+$	79	1
	Others		3	$(NO{\cdot}C_{10}H_{16})^+$	166	7	$C_6H_8^+$	80	2
				Others		4	$C_7H_8^+$	92	4
							$C_7H_9^+$	93	13
							$C_7H_{10}^+$	94	4
							$C_7H_{11}^+$	95	4
							$C_8H_{11}^+$	107	9
							$C_8H_{12}^+$	108	4
							$C_9H_{13}^+$	121	44
							$C_{10}H_{16}^+$	136	9
							Others		5

The branching ratios include all isotopes of each product. *m/z* values refer to the most abundant isotope of each product (pressure: 1.47 mbar, voltage ion inlet plate: −4 V, main carrier gas: He).

[a] Ionization energy of the monoterpene in eV from [42].

the signal of the product ion with $m/z = 81$ decreases at high monoterpene concentrations, whereas the one at $m/z = 137$ is still slightly rising. Therefore, secondary clustering may disturb the reaction product distribution somewhat. It is estimated, however, that with the reactant flows used at the inlet close to the inlet plate, the formation of secondary products should not shift the branching ratios of the products at $m/z = 137$ and 81 by more than 2%.

In a recent study, Tani et al. [15] have investigated in detail the product distribution of the H_3O^+ reaction with α- and β-pinene, Δ^3-carene and limonene in a PTR-MS instrument. The major difference between these experiments and this work lies in the choice of the carrier gas (air in the case of Tani et al., He in our case) and the fact that in the PTR-MS experiments an electric field is applied. Therefore, the ions have a drift velocity, defined by the magnitude of the applied electric field (E) and the number density N of the neutrals in the drift tube, and thus an enhanced energy. In our case, the ions are very rapidly thermalized in the flow tube. The fragmentation patterns of the H_3O^+ reactions in the PTR-MS were observed to vary with varying E/N. As E/N was decreased the percentage of the product with $m/z = 137$ was increased for each monoterpene, reaching values between 80 and 94% at the lowest values of E/N (80 Td).

The difference between these results and the data reported here are due to the applied electric field and the nature of the carrier gas in the flow tube. To investigate the possible influence of electric fields in our case, the influence of the voltage applied on the ion inlet plate has been examined for the H_3O^+/limonene and the H_3O^+/α-pinene reactions. Negligible effect is observed for voltages ranging from −4 up to −1 V. When the voltage is lowered to −7 V, the branching ratio of the protonated terpene ($m/z = 137$) decreases by a few percent (5% for α-pinene). This can be due to a more efficient fragmentation of the $(C_{10}H_{17}^+)^*$ complex, as observed in the PTR-MS experiments by Tani et al. [15], and partially to possible break-up or less efficient formation (due to the lower residence time of the accelerated ions) of secondary product ions. All product distributions listed in Table 2 are measured with −4 V applied on the ion inlet plate.

The pressure dependence of the product distribution has been investigated in the case of the H_3O^+/limonene reaction. Increasing the He buffer gas flow from 67 to 200 STP $cm^3\ s^{-1}$ resulted in a pressure increase from 1 up to 2.93 mbar. The branching ratio of the protonated monoterpene increased by 13%, whereas the branching ratio of the fragment ions with $m/z = 81$ and 95 decreased by 12 and 1%, respectively.

From the observations described above, it is clear that, if the product distribution is used for the analysis of chemical ionization mass spectrometry (CIMS) data, this distribution should be determined under the same operating conditions (pressure, applied voltage on the inlet plate, nature of buffer gas, ...) as those used in the CIMS experiment itself.

3.2.2. NO^+ reactions

For the reaction of NO^+ with the six monoterpenes, studied here, the major product is the ionized monoterpene $C_{10}H_{16}^+$ ($m/z = 136$), formed through charge transfer. Charge transfer with ground state NO^+ is possible for molecules with ionization energy (IE) smaller than the one of NO (IE = 9.26 eV [42]).

This condition is fulfilled for the four monoterpenes (α-pinene, limonene, Δ^3-carene, and camphene) for which the IE is known (see Table 2). Considering the trends in properties of hydrocarbons, it is reasonable to assume that the IE of all the monoterpenes is smaller than 9.26 eV. The occurrence of the parent cation $C_{10}H_{16}^+$ in the spectra of the reaction products of NO^+ with β-pinene and myrcene as the major peak supports this assumption and indicates that the IE of these compounds must also be smaller than the one of NO.

Some minor products ($m/z = 80$, 92, 93, 94, 121, and 135) are also observed. The latter are formed by partial fragmentation of the nascent $(C_{10}H_{16}^+)^*$ excited ion.

Striking is the relatively high branching ratio of the fragment ion with $m/z = 93$ for the non-cyclic monoterpene myrcene. In view of the low purity of the commercially available compound used here, we cannot exclude that this ion is due to impurities.

For all NO^+ reactions, the association product at $m/z = 166$, formed through

$$NO^+ + C_{10}H_{16} + He \rightarrow (NO \cdot C_{10}H_{16})^+ + He, \qquad (7)$$

is also observed (albeit with a branching ratio below 1% for the NO^+/β-pinene reaction).

The branching ratio of the association product for the NO^+/camphene reaction is relatively high (7%) in comparison with that observed for the other monoterpenes, which is in reasonable agreement with the observations made by Wang et al. [20], who report a 1–3% product at $m/z = 166$ for monoterpenes other than camphene and a 9% branching ratio for $(NO{\cdot}C_{10}H_{16})^+$ for camphene. This higher abundance of the association product $(NO{\cdot}C_{10}H_{16})^+$ in the case of camphene may be due to "charge transfer complexing" [44,45], by which the positive charge is more equally shared around the intermediate excited adduct ion. This process is considered to enhance the lifetime of this intermediate and thus the probability of a stabilizing collision with carrier gas atoms against dissociation. Charge transfer complexing is more efficient when the IE of NO and the one of the reactant molecule are not very different. This could be the case for camphene if the IE of camphene is close to the upper limit given in Table 2.

3.2.3. O_2^+ reactions

Since the IE of O_2 exceeds the one of NO by ∼3 eV, charge transfer between the monoterpenes and O_2^+ seems evident in view of the previous observations. However, as can be seen from Table 2, the parent ion $C_{10}H_{16}^+$ is not the most abundant product anymore. The charge transfer is suf-

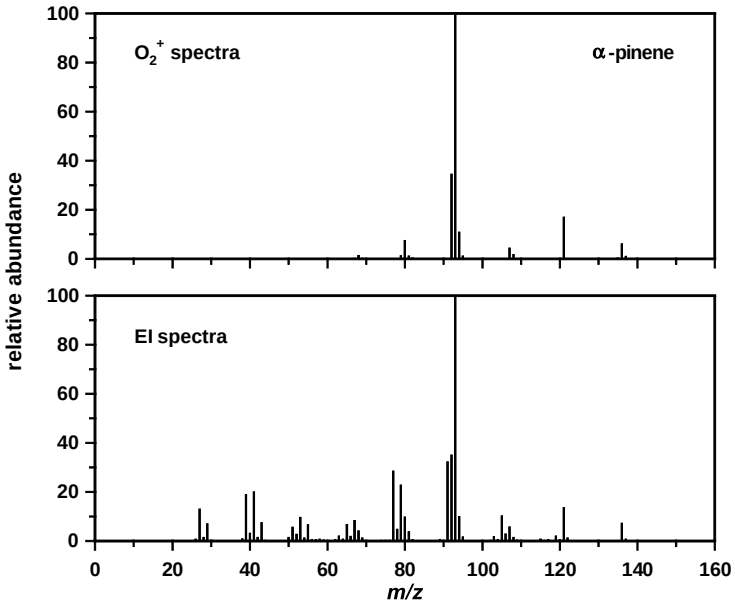

Fig. 4. Comparison between the O_2^+ spectra and the 70 eV EI spectra [42] of α-pinene.

ficiently exothermic to allow for cleavage of specific bonds in the nascent $(C_{10}H_{16}^+)^*$ exited parent cation, resulting in multiple fragment ions.

For all O_2^+ reactions, except for the reaction with camphene, the major product ion has $m/z = 93$. The O_2^+/camphene reaction mainly results in a product ion with $m/z = 121$. For the latter a CH_3^- ion transfer reaction can not be positively ruled out [24].

Comparison of the product distribution spectra of the O_2^+ reactions with the corresponding electron impact (EI) spectra from the NIST database [42], shows that the EI spectra contain more fragment ions (reaction with O_2^+ is a "softer" ionization), but albeit with different intensities, all products observed in the O_2^+ reaction spectra are also present in the corresponding EI spectra.

Figs. 4 and 5 show a comparison of the O_2^+ and EI spectra of α-pinene and myrcene, respectively.

In making such comparisons for the six monoterpenes studied here, some common features can also be noticed:

- Ions with $m/z = 121$ are the major product ions for the O_2^+/camphene reaction, in contrast with the other

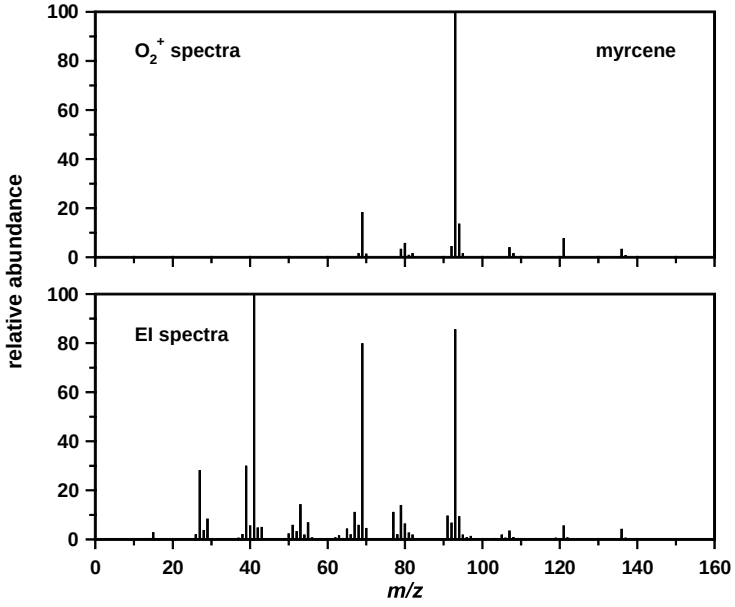

Fig. 5. Comparison between the O_2^+ spectra and the 70 eV EI spectra [42] of myrcene.

O_2^+/monoterpene reactions. These ions are also relatively more frequent in the EI spectra of camphene than in the other EI spectra.

- In the O_2^+/myrcene reaction spectra, the product with $m/z = 69$ has a higher branching ratio than in the other O_2^+ spectra, which is also observed in the EI spectra.
- Product ions with $m/z = 68$ are relatively more frequent in the O_2^+/limonene spectra than in the other O_2^+ spectra. This is also the case in the EI spectra of limonene, where they are the major products.

4. Conclusion

The reactions of H_3O^+, NO^+, and O_2^+ with the monoterpenes α-pinene, β-pinene, limonene, Δ^3-carene, myrcene, and camphene are fast and proceed within the experimental error at the collision rate.

In the case that only one monoterpene is involved, e.g., in specific laboratory experiments, H_3O^+, NO^+, and O_2^+ can be used as precursor ions for the derivation of the concentration of this monoterpene from CIMS measurements, provided that the product distribution of the reaction of the source ion with the monoterpene has been determined under the same operating conditions as the CIMS experiment itself.

In the case of a mixture of monoterpenes, the concentration of each constituent cannot be derived from CIMS spectra, since the reaction of H_3O^+ (NO^+ and O_2^+, respectively) with each of the six monoterpenes, studied here, results, although with different branching ratios, in identical products. Only when an averaged rate constant (if the rate constants for the different constituents are not too different, which is the case for the monoterpenes studied here) and an averaged product distribution are used, an estimation of the concentration of the mixture is possible.

Acknowledgements

The authors are indebted to Prof. David Smith and Prof. Patrik Španěl for valuable hints and discussions during the construction of the SIFT instrument. This work was partly funded by the Belgian "Federal Office for Scientific, Technical and Cultural Affairs" within the framework of the "Scientific support plan for a sustainable development policy (SPSD 2)—Global change, ecosystems and biodiversity—Project EV/35/06".

References

[1] A. Guenther, P. Zimmerman, M. Wildermuth, Atmos. Environ. 28 (1994) 1197.
[2] C. Geron, R. Rasmussen, R.R. Arnts, A. Guenther, Atmos. Environ. 34 (2000) 1761.
[3] R. Janson, K. Rosman, A. Karlsson, H.-C. Hansson, Tellus 53B (2001) 423.
[4] A. Guenther, C.N. Hewitt, D. Erickson, R. Fall, C. Geron, T. Graedel, P. Harley, L. Klinger, M. Lerdau, W.A. McKay, T. Pierce, B. Scholes, R. Steinbrecher, R. Tallamraju, J. Taylor, P. Zimmerman, J. Geophys. Res. 100 (1995) 8873.
[5] J.J. Orlando, B. Nozière, G.S. Tyndall, G.E. Orzechowska, S.E. Paulson, Y. Rudich, J. Geophys. Res. 105 (2000) 11561.
[6] B.R. Larsen, D. Di Bella, M. Glasius, R. Winterhalter, N.R. Jensen, J. Hjorth, J. Atmos. Chem. 38 (2001) 231.
[7] A. Reissell, C. Harry, S.M. Aschmann, R. Atkinson, J. Arey, J. Geophys. Res. 104 (1999) 13869.
[8] A. Römpp, B. Bonn, G.K. Moortgat, R. Winterhalter, R. Van Dingenen, M. Spittler, K. Wirtz, Proceedings of the 8th European Symposium on the Physico-Chemical Behaviour of Atmospheric Pollutants, 17–20 September 2001, Torino, Italy, extended abstract TP24, CD ROM, 2002.
[9] S. Hayward, R.J. Muncey, A.E. James, C.J. Halsall, C.N. Hewitt, Atmos. Environ. 35 (2001) 4081.
[10] V. Van den Bergh, H. Coeckelberghs, I. Vanhees, R. De Boer, F. Compernolle, C. Vinckier, Anal. Bioanal. Chem. 372 (2002) 630.
[11] C. Warneke, T. Karl, H. Judmaier, A. Hansel, A. Jordan, W. Lindinger, P.J. Crutzen, Global Biogeochem. Cycles 13 (1999) 9.
[12] R. Holzinger, L. Sandoval-Soto, S. Rottenberger, P.J. Crutzen, J. Kesselmeier, J. Geophys. Res. 105 (2000) 20573.
[13] A. Wisthaler, N.R. Jensen, R. Winterhalter, W. Lindinger, J. Hjorth, Atmos. Environ. 35 (2001) 6181.
[14] W. Lindinger, A. Hansel, A. Jordan, Int. J. Mass Spectrom. Ion Process. 173 (1998) 191.
[15] A. Tani, S. Hayward, C.N. Hewitt, Int. J. Mass Spectrom. 223/224 (2003) 561.
[16] C. Amelynck, N. Schoon, J. Riondato, E. Arijs, Geophysical Research Abstracts 5, EGS-AGU-EUG Joint Assembly, 6–11 April 2003, Nice, France, abstract number EAE03-A-02664, CD ROM.
[17] D. Smith, P. Španěl, Int. Rev. Phys. Chem. 15 (1996) 231.
[18] P. Španěl, A.M. Diskin, S.M. Abbott, T. Wang, D. Smith, Rapid Commun. Mass Spectrom. 16 (2002) 2148.
[19] D. Smith, T. Wang, J. Sulé-Suso, P. Španěl, A. El Haj, Rapid Commun. Mass Spectrom. 17 (2003) 845.
[20] T. Wang, P. Španěl, D. Smith, Int. J. Mass Spectrom. 228 (2003) 117.
[21] D. Smith, N.G. Adams, Adv. Atom. Mol. Phys. 24 (1988) 1.
[22] N.G. Adams, D. Smith, Int. J. Mass Spectrom. Ion Phys. 21 (1976) 349.
[23] P. Španěl, Y. Ji, D. Smith, Int. J. Mass Spectrom. Ion Process. 165/166 (1997) 25.
[24] P. Španěl, D. Smith, Int. J. Mass Spectrom. Ion Process. 167/168 (1997) 375.
[25] P. Španěl, D. Smith, Int. J. Mass Spectrom. Ion Process. 172 (1998) 137.
[26] P. Španěl, D. Smith, Int. J. Mass Spectrom. Ion Process. 172 (1998) 239.
[27] P. Španěl, D. Smith, Int. J. Mass Spectrom. 176 (1998) 167.
[28] P. Španěl, D. Smith, Int. J. Mass Spectrom. 176 (1998) 203.
[29] P. Španěl, D. Smith, Int. J. Mass Spectrom. 181 (1998) 1.
[30] P. Španěl, D. Smith, Int. J. Mass Spectrom. 185–187 (1999) 139.
[31] P. Španěl, D. Smith, Int. J. Mass Spectrom. 189 (1999) 213.
[32] P. Španěl, J.M. Van Doren, D. Smith, Int. J. Mass Spectrom. 213 (2002) 163.
[33] A.M. Diskin, T. Wang, D. Smith, P. Španěl, Int. J. Mass Spectrom. 218 (2002) 87.
[34] P. Španěl, T. Wang, D. Smith, Int. J. Mass Spectrom. 218 (2002) 227.
[35] T. Wang, D. Smith, P. Španěl, Rapid Commun. Mass Spectrom. 16 (2002) 1860.
[36] P. Španěl, D. Smith, Int. J. Mass Spectrom. 184 (1999) 175.
[37] T. Su, W.J. Chesnavich, J. Chem. Phys. 76 (1982) 5183.
[38] T. Su, J. Chem. Phys. 89 (1988) 5355.

[39] M.T. Fernandez, C. Williams, R.S. Mason, B.J. Costa Cabral, J. Chem. Soc. Faraday Trans. 94 (1998) 1427.
[40] P. Španěl, D. Smith, J. Am. Soc. Mass Spectrom. 12 (2001) 863.
[41] M.J. Frisch, G.W. Trucks, H.B. Schlegel, G.E. Scuseria, M.A Robb, J.R. Cheeseman, V.G. Zakrzewski, J.A. Montgomery Jr., R.E. Stratmann, J.C. Burant, S. Dapprich, J.M. Millam, A.D. Daniels, K.N. Kudin, M.C. Strain, O. Farkas, J. Tomasi, V. Barone, M. Cossi, R. Cammi, B. Mennucci, C. Pomelli, C. Adamo, S. Clifford, J. Ochterski, G.A. Petersson, P.Y. Ayala, Q. Cui, K. Morokuma, D.K. Malick, A.D. Rabuck, K. Raghavachari, J.B. Foresman, J. Cioslowski, J.V. Ortiz, A.G. Baboul, B.B. Stefanov, G. Liu, A. Liashenko, P. Piskorz, I. Komaromi, R. Gomperts, R.L. Martin, D.J. Fox, T. Keith, M.A. Al-Laham, C.Y. Peng, A. Nanayakkara, C. Gonzalez, M. Challacombe, P.M.W. Gill, B. Johnson, W. Chen, M.W. Wong, J.L. Andres, C. Gonzalez, M. Head-Gordon, E.S. Replogle, J.A. Pople, Gaussian 98, Revision A.7, Gaussian Inc., Pittsburgh, PA, 1998.
[42] P.J. Linstrom, W.G. Mallard (Eds.), NIST Chemistry WebBook, NIST Standard Reference Database Number 69, July 2001, National Institute of Standards and Technology, Gaithersburg, MD (http://webbook.nist.gov).
[43] P. Španěl, D. Smith, Rapid. Commun. Mass Spectrom. 13 (1999) 585.
[44] E.E. Ferguson, D. Smith, N.G. Adams, J. Chem. Phys. 81 (1984) 742.
[45] P. Španěl, D. Smith, J. Chem. Phys. 104 (1996) 1893.